Identification of Intracellular Phospholipases A_2 in the Human Eye: Involvement in Phagocytosis of Photoreceptor Outer Segments

Miriam Kolko,[1,2,3] *Jinmei Wang,*[1,3,4] *Chen Zhan,*[1,3] *Kristian A. Poulsen,*[5] *Jan Ulrik Prause,*[1] *Mogens Holst Nissen,*[3] *Steffen Heegaard,*[1] *and Nicolas G. Bazan*[6]

Purpose. To identify intracellular phospholipases A_2 (PLA_2) in the human retina and to explore the role of these enzymes in human retinal pigment epithelium (RPE) phagocytosis of photoreceptor outer segments (POS).

Methods. PCR amplification and Western blot analysis were used to identify mRNA and protein expression of intracellular PLA_2 subtypes in the retinal pigment epithelial cell line ARPE-19. Immunohistochemical staining of normal human eye sections was performed to reveal the cellular location of the enzymes. A model of RPE phagocytosis of POS was used to explore the role of intracellular PLA_2 in phagocytosis. An activity assay was used to evaluate PLA_2 activity, and inhibitors of specific PLA_2 were applied to evaluate the role of PLA_2 in RPE phagocytosis.

Results. Genes encoding calcium-independent (i)PLA_2, group VIA; calcium-dependent cytosolic (c)PLA_2, groups IVA, IVB, and IVC; and iPLA_2, group VIB, were identified in the human RPE cell line ARPE-19. Furthermore, protein of iPLA_2-VIA, cPLA_2-IVA, and iPLA_2-VIB were identified in ARPE-19 cells and in various parts of the normal human eye. iPLA_2-VIA protein levels were upregulated during phagocytosis, and iPLA_2-VIA activity was found to be specifically increased 12 hours after ARPE-19 cells were fed with POS. Finally, RPE phagocytosis was inhibited by the iPLA_2-VIA inhibitor bromoenol lactone.

Conclusions. Various intracellular PLA_2 subtypes are present in the human retina. iPLA_2-VIA may play an important role in the regulation of RPE phagocytosis of POS and may also be involved in the regulation of photoreceptor cell renewal.

From the [1]Eye Pathology Institute, the [3]Department of Medical Anatomy, The Panum Institute, and the [5]Institute of Molecular Biology and Physiology, University of Copenhagen, Copenhagen, Denmark; the [2]Department of Ophthalmology, Glostrup University Hospital, Copenhagen, Denmark; the [4]Department of Ophthalmology, Second Clinical Hospital, Jilin University, Changchun, Peoples Republic of China; and the [6]Neuroscience Center of Excellence and Department of Ophthalmology, Louisiana State University Health Sciences Center School of Medicine, New Orleans, Louisiana.

Supported by the Hørslev Fonden, The Danish Eye Research Foundation, The Danish Eye Health Society, the Augustinus Fonden, the Fam. Hede Nielsens Fond, the Dir. Ib Henriksens Fond, Civilingeniør Lars Andersens Legat, the Alice and Jørgen A. Rasmussens Mindelegat, Chr. Andersen and hustru Ingeborg Andersen, f. Schmidts legat, and National Eye Institute Grant EY05121.

Submitted for publication July 26, 2006; revised November 2, 2006; accepted January 22, 2007.

Disclosure: **M. Kolko**, None; **J. Wang**, None; **C. Zhan**, None; **K.A. Poulsen,** None; **J.U. Prause**, None; **M.H. Nissen**, None; **S. Heegaard**, None; **N.G. Bazan**, None

The publication costs of this article were defrayed in part by page charge payment. This article must therefore be marked "*advertisement*" in accordance with 18 U.S.C. §1734 solely to indicate this fact.

Corresponding author: Miriam Kolko, Eye Pathology Institute, Frederik d. V's vej 11, 1st floor, 2100 Copenhagen, Denmark; mkolko@dadlnet.dk.

(*Invest Ophthalmol Vis Sci.* 2007;48:1401–1409) DOI: 10.1167/iovs.06-0865

The retinal pigment epithelium (RPE) is essential to maintaining a functional neuroretina. One of the most important functions of RPE is to phagocytize the shed tip of photoreceptor cells. During this process, photoreceptor outer segments (POS) are constantly formed at the base of the POS and are phagocytized by the adjacent RPE in a tightly regulated intracellular signaling pathway coupling phagocytosis with expression of POS-degradative enzymes.[1] The essential role of RPE phagocytosis is highlighted by the rapid degeneration of photoreceptors in Royal College of Surgeon's rats, which carry an autosomal recessive mutation that impairs RPE phagocytosis, resulting in subretinal accumulation of POS.

Phospholipids (PLs) represent major constituents of POS. Published values for the percentage of PL in bovine POS varies between 30% and 60%, depending on the procedure for POS preparation.[2,3] Phosphatidylcholine (PC) and phosphatidylethanolamine (PE) account for 80% of the PL in POS; followed by phosphatidylserine with 13%; and finally by phosphatidylinositol, sphingomyelin, and lipids in the solvent (phosphatidic acid, phosphatidylglycerol, diphosphosphatidylglycerol, and dipalmitoylphosphatidylethanolamine), which makes up the rest.[4,5]

Even though recent studies emphasize the differences between macrophage and RPE phagocytosis, the two processes show many similarities, and much can be learned from macrophage studies to further our understanding of RPE phagocytosis.[6] Among other mediators of phagocytosis. phospholipases A_2 (PLA_2) have been found to be involved in macrophage engulfment.[7–9] PLA_2 is a group of enzymes catalyzing the hydrolysis of *sn*-2 fatty acyl chains, thereby releasing free fatty acids and lysophospholipids. PLA_2 can be divided into various groups according to their cellular location, calcium dependency, and substrate specificity. The most recent classifications divide PLA_2 into high-molecular-weight cytosolic calcium-dependent (c)PLA_2, groups IVA, IVB, IVC, and IVD; high-molecular-weight calcium-independent (i)PLA_2, groups VIA and VIB; low-molecular-weight secretory (s)PLA_2, groups IB, IIA, IIC, IID, IIE, IIF, III, V, X, and XIIA; and the substrate-specific platelet-activating factor-acetylhydrolases (PAF-AH), groups VIIA, VIIB, VIIIA, and VIIIB.[10–12] Macrophage studies have revealed involvement of cyclooxygenases (COX) and prostaglandins as a result of PLA_2 activity in the regulation of phagocytosis.[8,13,14] Most evident is the role of cPLA_2 and sPLA_2, group V in regulation of phagocytosis.[7,15] Recent studies furthermore indicate a role of iPLA_2 in phagocytosis since PLA_2-induced cleavage of PC in dying cells leads to phagocytosis of these by adjacent macrophages.[9] There is only limited evidence of the involvement of PLA_2 in RPE phagocytosis. However, RPE has been shown to elicit PLA_2 activity,[16,17] and RPE phagocytosis of POS has been shown to induce prostaglandins by COX activation.[18] Preliminary findings have revealed the highest abundance of the high-molecular-weight PLA_2 in the

Copyright © Association for Research in Vision and Ophthalmology

Downloaded from iovs.arvojournals.org on 04/13/2021

TABLE 1. RT-PCR Primers Used for PCR Cloning of Intracellular PLA_2 Subtypes

Gene and Accession No.			Primer Sequences 5′–3′	Product (bp)
Human $iPLA_2$-VIA all	NM_001004426.1	1440–1459:	CAG GGC TCT GCA GCG CCA CAT CAT	294
		1715–1734:	GTC CCT GTC AGC ATC ACC TT	
Human $iPLA_2$-VIA +/− exon 9	NM_003560.2	1244–1263:	ATC GTG TTC GGA GCA GAA GT	384
		1609–1628:	TGA GGA GCT GGAT GAT GAT G	
Human $iPLA_2$-VIA Larsson et al.	NM_003560.2	1409–1432:	CAG GGC TCT GCA GCG CCA CAT CAT	236
		1622–1645:	GGC CTT CTC GAT GGC GAT GAG GAG	
Human $iPLA_2$-VIA +/− exon 4	NM_003560.2	137–157:	ATG ATG TGG CGC TGC AGA GCC CTG	1295
		1409–1432:	ATG CAG TTC TTT GGC CGC CTG	
Human $cPLA_2$-IVA	BC114340	545–564:	TGG CTC TGT GTG ATC AGG AG	300
		826–845:	GGC CCT TTC TCT GGA AAA TC	
Human $cPLA_2$-IVB	DQ523800.1	705–724:	GAG AAG GCA GAG GTG TCC AG	179
		865–884:	TTC CAG ACA GGG CTA CTG CT	
Human $cPLA_2$-IVC	NM_003706.1	490–509:	GGG GTC CTG AGT GAG ATG AA	366
		836–856:	GGA AGG TTG CAG GTC ATT GT	
Human $cPLA_2$-IVD	AB090876.1	216–235:	TTG AGT GAG GGC CGA CCC TTA	323
		520–539:	TGG GCG ATC TGA CGT TTC TT	
Human $iPLA_2$-VIB	AF263613	2035–2055:	GCC ATT AGA GCC TCA TCT GC	301
		2317–2336:	TCA GGA GGT AAC AGG CCA TC	

human RPE cell line ARPE-19 compared with the low-molecular-weight $sPLA_2$. The present study therefore evaluated the known high-molecular-weight PLA_2 in human RPE cells and explored their possible role in ARPE-19 phagocytosis of POS.

METHODS

ARPE-19 Cultures

Human ARPE-19 cells (purchased from ATTC-LGC Promochem AB, Boras, Sweden) were maintained at 37°C in a humidified chamber of 5% CO_2 in Dulbecco's modified Eagle's medium- F12 (DMEM) containing 5 mM glucose and supplemented with 15% fetal bovine serum (FBS), 100 U/mL penicillin, and 100 μg/mL streptomycin (Invitrogen-Gibco, Carlsbad, CA). The cells were grown in six-well plates, and the culture medium was replaced with fresh medium twice a week. The cells were harvested at different time points and kept at −80°C until use.

PCR Amplification

Total RNA was extracted from 2-week-old ARPE-19 cultures. cDNA was then generated (ThermoScript cDNA kit; Invitrogen-Gibco). One microgram of total RNA was used for each reaction with polyT primers and amplified (AmpliTaqGold; (Applied Biosystems, Foster City, CA). To exclude genomic contamination, controls were made by excluding the polyT primers during reverse transcription. Furthermore, primer sets were all designed to span an intron. Volumes of cDNA used were 5 μL (from 100 ng RNA) for each of the PLA_2s. Amplification was performed in an automated thermal cycler (model 2400; Perkin Elmer, Boston, MA). Primers were as outlined in Table 1. PCR products were ligated into PCR-II vectors (Invitrogen-Gibco) and sequenced, thereby confirming the specificity of the PCR reactions.

Western Blot Analysis

ARPE-19 cells were kept in growth medium and incubated with POS or PBS. The cells were collected after 12 and 24 hours and homogenized in 500 μL lysis buffer. Samples were centrifuged at 4000*g* for 25 minutes at 4°C, and samples containing 25 μg protein were loaded. Blots were preincubated overnight in TBS (0.2 mM Tris-HCl [pH 7.5], 150 mM NaCl, 0.1% Tween 20) containing 5% nonfat dry milk and incubated with one of the following primary antibodies in TBS-1% bovine serum albumin for 3 hours at room temperature: $iPLA_2$-VIA (CAY-160507, 1:500; Cayman Chemical, Ann Arbor, MI); $cPLA_2$-IVA (SC-454, 1:500; Santa Cruz Biotechnology, Santa Cruz, CA); or $iPLA_2$-VIB (1:100), prepared as described by Poulsen et al. (manuscript submitted). Extracellular signal-regulated kinase (ERK) expression did not change during phagocytosis and blots incubated with an antibody recognizing ERK were used as loading controls (see Fig. 4B). Blots were washed in TBS and incubated with goat anti-rabbit IgG alkaline phosphatase secondary antibody (TriChem ApS; Interkemi, Frederikssund, Denmark) followed by visualization using BCIP/NBT (5-bromo-4-chloro-3-indoyl phosphate-nitroblue tetrazolium) substrate (VWR International ApS, Albetslund, Denmark).

Immunoprecipitation

Protein was isolated from 3-week-old ARPE-19 cells as just described. Precleared supernatant was incubated with a goat anti-$iPLA_2$-VIA antibody (SC-14463; 1:400; Santa Cruz Biotechnology, Inc.) overnight at 4°C. To monitor nonspecific binding, we omitted the antibody from a similar sample. After incubation, 50 μL of protein G-Sepharose beads (GE Healthcare, Hillerød, Denmark) was added, and samples were incubated at 4°C for a further 4 hours. The resin was collected by centrifugation and washed five times in buffer. Bound protein was eluted by boiling the resin in 40 μL of 2× loading buffer and resolved by SDS gel electrophoresis. Blots were stained with a rabbit anti-$iPLA_2$-VIA (CAY-160507, 1:200; Cayman Chemical).

Immunohistochemistry

Human eyes were obtained from the Eye Pathology Institute, University of Copenhagen, in accordance with the guidelines of the Declaration of Helsinki for research involving human tissue. Sections were deparaffinized, boiled for 20 minutes in a microwave in TE buffer (pH = 9.5) for antigen retrieval and incubated with 3% H_2O_2 for 8 minutes at room temperature, to inhibit endogenous peroxidase activity. Sections were exposed to antibodies that specifically recognize $iPLA_2$-VIA (1:200), $iPLA_2$-VIB (1:200), or $cPLA_2$-IVA (1:200); washed twice with PBS; and exposed to biotinylated anti-rabbit IgG followed by incubation with a dilution of streptavidin peroxidase complex reagent and finally visualized by the use of AEC (3-amino-9-ethylcarbazole) chromogen (Dako Inc., Copenhagen, Denmark). Relevant positive and negative controls were used. Immunostained sections were examined by light microscopy.

Confocal Microscopy

ARPE-19 cells were detached with trypsin, transferred to glass coverslips in 24-well plates, and incubated in normal glucose medium. The cells were grown to confluence and stained with an $iPLA_2$-VIA-specific antibody (SC-160507; 1:200) overnight at 4°C. They were washed three times with PBS and fixed in formaldehyde 3.7% for 15 minutes at

Downloaded from iovs.arvojournals.org on 04/13/2021

room temperature, followed by membrane permeabilization by 0.2% Triton X-100 in TBS for 10 minutes. They were washed three times in blocking buffer (TBS+5% BSA), and Alexa 488-phalloidin (1:20; Invitrogen-Gibco) was added to for 2 hours at room temperature in the dark. Finally, the cells were washed three times in blocking buffer. Coverslips were moved to slides and sealed with fluorescence-preserving mounting medium (Vector Laboratories, Burlingame, CA). A confocal laser scanning image system (LSM 510; Carl Zeiss Meditec GmbH, Düsseldorf, Germany) was used to detect immunofluorescence.

Isolation of POS

Normal bovine eyes were obtained from an abattoir, and preparation was initiated within 6 hours after enucleation. POS isolation was performed as described by Hall.[1] The retina was removed and transferred into PBS. The retinal tissue was trypsinized on ice and fragmented by a magnetic stirrer for 30 minutes. Large tissue fragments were eliminated by precipitation for 20 minutes at 4°C, and supernatants were centrifuged at 800*g* for 10 minutes. The samples were rinsed twice with PBS, and aliquots containing 40×10^6 POS were stored at −70°C until use.

Labeling of POS and Quantification of POS Phagocytosis by ARPE-19 Cells

POS were labeled with the biotin-streptavidin method described by Schraermeyer and Stieve.[19] POS suspended in PBS were centrifuged at 1000*g* for 10 minutes. The pellet, containing the outer segments, was then biotinylated with 1:5 (wt/vol) 0.8 mg/mL NHS-LC biotin (Sigma-Aldrich, St. Louis, MO) dissolved in PBS for 1 hour in the dark and on ice. POS was washed twice in PBS and in a second step, the biotin residues on the outer segments were labeled 1:5 (wt/vol) with 0.05 mg/mL streptavidin-AlexaFluor568 red (Jackson ImmunoResearch, West Grove, PA) for 1 hour in the dark and on ice and washed twice in PBS to remove unbound conjugates. Finally, POS was resuspended 1:2 (wt/vol) in PBS. RPE cells were grown in 96-well plates. Media were removed, and 200 μL of Locke's solution (154 mM NaCl, 5.6 mM KCl, 10 mM glucose, 2.2 mM $CaCl_2$, and 5 mM HEPES buffer adjusted to pH 7.4) was added to all wells. Five microliters POS was gently added on top of confluent monolayer cultures of ARPE-19 cells grown in 96-well plates. Five microliters of Locke's was added to the control wells. Incubations were continued in darkness for various time intervals at 37°C in an atmosphere of 5% CO_2 and 95% air. Phagocytized fluorescent POS were detected with a gel and blot imager (Typhoon 9410; GE Healthcare) equipped with a 532-nm excitation filter. Background fluorescence of the system, as assayed without cells, was very low and was automatically subtracted. Bromoenol lactone (BEL; 0.1. 1, 5, 10, or 20 μM), arachidonyl trifluoromethyl ketone (AACOCF3; 10 μM) or propranolol (150 μM) was added to cells simultaneously with the POS. To evaluate the phagocytosis of POS, we added Alexa-red-labeled POS to ARPE-19 cells grown on glass coverslips, as described earlier. After 12 hours, the cells were washed three times with PBS and fixed. Alexa 488-phalloidin (1:20; Invitrogen) was added to the cells for 2 hours at room temperature without light. Finally, the cells were washed and visualized with a confocal laser scanning image system.

Cytotoxicity Assay

After an overnight incubation with different concentrations of BEL ($n = 6$ for each condition) cell viability was determined by a colorimetric method, which is based on the conversion of yellow MTT salt (3-(4.5-dimethylthiazol-2-yl)-2.5-diphenyl tetrazolium bromide; Sigma-Aldrich) to an insoluble purple formazan dye by mitochondrial dehydrogenase of living cells. Briefly, the assay was performed by removing the cell culture medium and replacing it with 100 μL fresh culture medium containing 5.0 mg/mL MTT. After 4 hours of incubation at 37°C, the cells were solubilized overnight with 100 μL of a solution containing 50% dimethylformamide and 20% SDS (pH 4.7), and absorbance was measured at 560 nm. The background readings (blank wells with medium, MTT, and solubilization buffer) were subtracted from the average absorbance readings of the BEL-treated wells, to obtain an adjusted absorbance reading that represented cell viability. This reading was divided by the adjusted absorbance reading of untreated cells in control wells, to obtain the percentage of cell survival.

Measurement of PLA_2 Activity

ARPE-19 cells, with or without preincubation with POS, were collected and homogenized in 150 μL lysis buffer (50 mM HEPES, 1 mM EDTA, 1 mM Na-orthovanadate, and protease inhibitor cocktail [1:100; Sigma-Aldrich]). Samples were centrifuged at 2000*g* for 30 minutes at 4°C. The supernatants were collected and subsequently spun though 30-kDa cutoff filters (12 minutes, 14,000*g*; Microcon YM-30; Millipore, Hundested, Denmark). Arachidonoyl thio-PC was used as a synthetic substrate to detect PLA_2 activity. Hydrolysis of the arachidonoyl thioester bond at the *sn*-2 position by PLA_2 releases free thiol, which is detected by Ellman's reagent. PLA_2 activity was determined in the supernatant with a $cPLA_2$ assay kit (Cayman Chemical), in the presence and absence of a specific inhibitor of $iPLA_2$, BEL, which was incubated for 15 minutes at 25°C at a concentration of 10 μM before the assay. Activity was calculated by measuring the absorbance at 405 nm, using the 5.5′-dithiobis(2-dinitrobenzoic acid; DTNB) extinction coefficient of 10.66/mM, and reported as nanomoles per minute per gram cytosolic protein.

Statistics

Quantitative results are expressed as the mean ± SD. Statistical significance between experimental groups was assessed by Student's *t*-test.

Results

Expression of mRNAs and Proteins of Intracellular PLA_2s in ARPE-19 Cells

Primers recognizing genes encoding $iPLA_2$-VIA, $cPLA_2$-IVA, and $iPLA_2$-VIB revealed significantly higher expression of $iPLA_2$-VIA than of $cPLA_2$-IVA and $iPLA_2$-VIB. $cPLA_2$-IVA ($P < 0.001$, $n = 4$) and $iPLA_2$-VIB ($P < 0.001$, $n = 4$) mRNA expression was 12% and 67% of $iPLA_2$-VIA mRNA expression ($n = 4$), respectively (Fig. 1A). RT-PCR primers designed to detect splice variants of $iPLA_2$-VIA documented the expression of the known alternative genes encoding the $iPLA_2$-VIA region, with and without exon 9, ankyrin 1, and ankyrin 2.[20] We furthermore identified a new splice variant containing intron 4 (Fig. 1B). Finally, primers specifically recognizing $cPLA_2$-IVA, $cPLA_2$-IVB, or $cPLA_2$-IVC revealed mRNA expression of these genes in ARPE-19 cells (Figs. 1A, 1B). A primer set recognizing $cPLA_2$-IVD did not amplify a product (not shown).

Western blot analysis, using antibodies against human $iPLA_2$-VIA, human $cPLA_2$-IVA, and human $iPLA_2$-VIB, revealed protein expression of all the intracellular PLA_2s in ARPE-19 cells. POS did not express any of the known PLA_2s (Fig. 2A). $iPLA_2$-VIA identified a ~85-kDa band and a ~70-kDa band, previously described in the literature.[21] The $cPLA_2$-IVA antibody recognized a ~100-kDa band and finally $iPLA_2$-VIB recognized a ~88, ~77, ~63, and ~48-kDa band. Immunohistochemical staining of ARPE-19 cells confirmed the protein expression of all the intracellular PLA_2s (Fig. 2B). The authenticity of the ~70-kDa protein to which the CAY-160507 (Cayman Chemical) antibody reacts, was evaluated by immunoprecipitation. An $iPLA_2$-VIA-directed antibody (SC-14463; Santa Cruz Biotechnology, Inc.) was used to immunoprecipitate $iPLA_2$-VIA from ARPE-19 cells. In this precipitate, both the ~85- and the ~70-kDa proteins were recognized by Western blot analysis using the CAY-160507 antibody, strongly indicating that this protein is an $iPLA_2$-VIA protein product (data not shown).

Downloaded from iovs.arvojournals.org on 04/13/2021

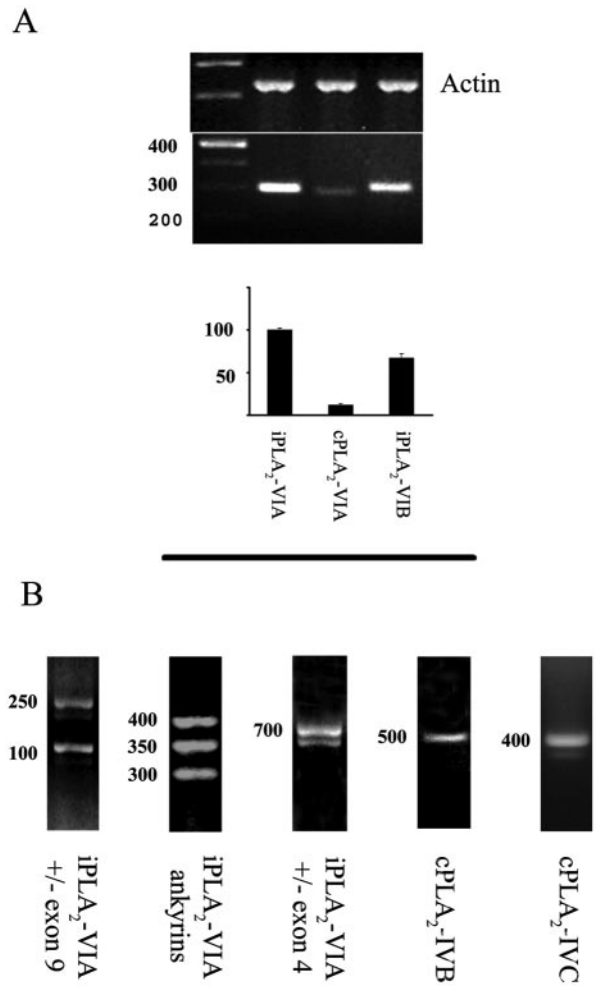

FIGURE 1. (**A**) PCR amplification and semiquantitative analysis of genes encoding iPLA$_2$-VIA, cPLA$_2$-IVA, and iPLA$_2$-VIB. (**B**) PCR amplification of genes encoding iPLA$_2$-VIA splice variants and cPLA$_2$-IV subtypes.

Cellular Location of Intracellular PLA$_2$ in the Normal Human Eye

Six normal eyes were used for evaluation of the expression pattern of intracellular PLA$_2$. Antibodies recognizing iPLA$_2$-VIA, cPLA$_2$-IVA, and iPLA$_2$-VIB were used as described in the Methods section. Table 2 presents the reactivity of the various ocular structures.

In the cornea, moderate detectable expression of iPLA$_2$-VIA was found in the epithelial cells, whereas strong iPLA$_2$-VIA expression was observed in the endothelium (Fig. 3A). Weak to moderate iPLA$_2$-VIA expression was found in the dilator and sphincter muscles. Pigmented and nonpigmented ciliary epithelial cells (Fig. 3B) as well as the ciliary muscle revealed moderate iPLA$_2$-VIA expression. Strong expression of iPLA$_2$-VIA was observed in various layers of the retina (Fig. 3C). The most abundant expression was detected in the RPE cells, the ganglion cells, and the nerve fiber layer. Moderate iPLA$_2$-VIA expression was found in the photoreceptor inner segment and the inner and outer plexiform layers, whereas no expression appeared in the nuclear layers and the POS (Figs. 2B, 3C). Moderate iPLA$_2$-VIA expression appeared in both the anterior (Fig. 3D) and equatorial lens epithelium.

cPLA$_2$-IVA expression also showed widespread expression in the human eye. In the cornea moderate detectable expression was found in the epithelial cells and in the endothelium (Fig. 3E). Pigmented epithelial cells of the ciliary body (Fig. 3F) as well as the ciliary muscle revealed moderate cPLA$_2$-IVA expression, whereas strong staining appeared in the nonpigmented epithelial cells (Fig. 3F). Moderate expression was detected in the photoreceptor inner segment of the retina (Fig. 3G). Weak expression of cPLA$_2$-IVA was found in the anterior (Fig. 3H) and equatorial lens epithelium.

In contrast to the expression of iPLA$_2$-VIA and cPLA$_2$-IVA, iPLA$_2$-VIB appeared both in the cytosol and the nuclei of various cells in the human eye. Strong iPLA$_2$-VIB was found in the corneal epithelium and moderate expression was detected in the corneal endothelium (Fig. 3I). Pigmented and nonpigmented epithelial cells of the ciliary body (Fig. 3J) and ciliary muscle revealed moderate iPLA$_2$-VIB expression. In the retina, moderate iPLA$_2$-VIB expression was found in the photoreceptor inner segment, the inner nuclei layer, in the ganglion cells, in the nerve fiber layer and in the RPE (Fig. 3K). Strong iPLA$_2$-VIB expression appeared in both the anterior (Fig. 3L)

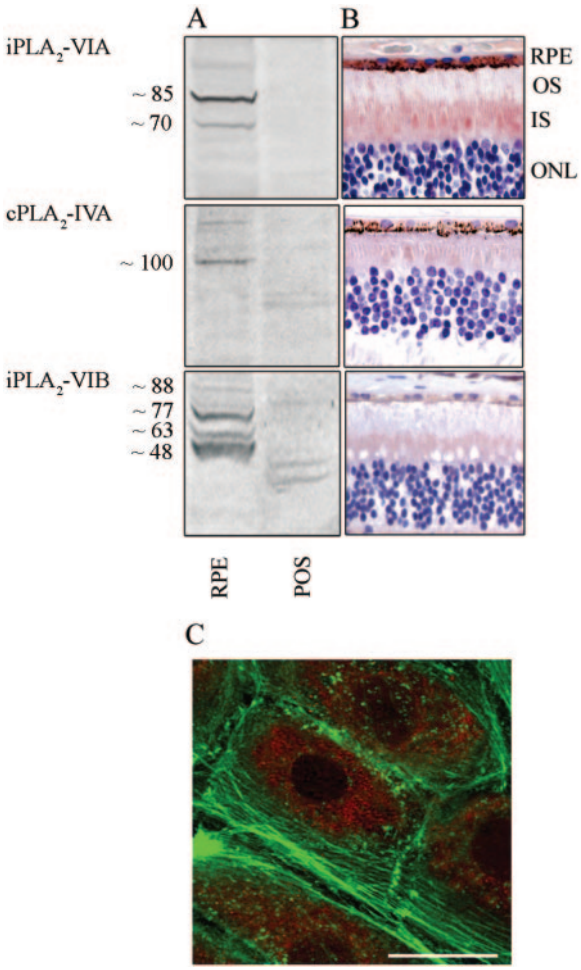

FIGURE 2. (**A**) Western blot analysis using iPLA$_2$-VIA-, cPLA$_2$-IVA-, and iPLA$_2$-VIB-specific antibodies on protein isolated from ARPE-19 cells and bovine POS. (**B**) Immunohistochemical staining of normal human retinas with antibodies specifically recognizing iPLA$_2$-VIA, cPLA$_2$-IVA, and iPLA$_2$-VIB. Note strong reactivity in the RPE with iPLA$_2$-VIA and only weak reactivity with the other two antibodies. RPE, retinal pigment epithelium; OS, photoreceptor outer segments; POS, photoreceptor outer segments; IS, photoreceptor inner segments; ONL, outer nuclear layer. (**C**) Immunohistochemical staining of ARPE-19 cells. *Red*: iPLA$_2$-VIA reactivity; *green*: cytoskeleton, stained by Alexa 488-phalloidin. Note the iPLA$_2$-VIA reactivity in the cytosol of the ARPE-19 cells. Bar, 5 μm.

Downloaded from iovs.arvojournals.org on 04/13/2021

TABLE 2. Staining Intensity of $iPLA_2$-VIA, $cPLA_2$-IVA, and $iPLA_2$-VIB Protein Expression in the Human Eye

Tissue	$iPLA_2$-VIA	$cPLA_2$-VIA	$iPLA_2$-VIB
Sclera	−	−	−
Cornea			
Epithelium	++	++	++++
Stromal keratocytes	−	−	−
Endothelium	+++	++	++
Trabecular meshwork	−	−	−
Iris			
Stroma	−	−	−
Dilator muscle	++	+	+++
Sphincter muscle	++	+	+++
Anterior iris epithelium	+	−	+
Posterior iris epithelium	+	−	+
Ciliary body			
Nonpigmented epithelium	++	+++	++
Pigmented epithelium	++	++	++
Ciliary muscle	++	+	++
Choroid			
Endothelial cells	−	−	−
Fibrocytes	−	−	−
Melanocytes	+	−	−
Retina			
Internal limiting membrane	−	−	−
Nerve fiber layer	+++	+	++
Ganglion cell layer	+++	+	++
Inner plexiform layer	+	−	+
Inner nuclear layer	−	−	++
Outer plexiform layer	+	−	+
Outer nuclear layer	−	−	−
External limiting membrane	−	−	+
Photoreceptor inner segments	++	++	++
Photoreceptor outer segments	−	+	−
Retinal pigment epithelium	++++	+	++
Glial cells	−	−	−
Optic nerve			
Axons	+++	+	++
Glial cells	−	−	−
Lens			
Anterior lens epithelium	++	+	+++
Equatorial lens epithelium	+	+	+++
Lens fibers	−	−	−

* The staining intensity was scored as negative (−), weak (+), moderate (++), strong (+++), or very strong (++++). The intensity shown is an average of results in six normal eyes.

and equatorial lens epithelium. In control eyes stained with rabbit serum, no reactivity appeared (Fig. 3M). In control eyes stained with preimmune serum from the rabbits used to produce the $iPLA_2$-VIB antibody, weak reactivity appeared in the photoreceptor inner segment, in the inner and outer plexiform layers, and in the nerve fiber layer (Fig. 3N).

Cellular Location of $iPLA_2$-VIA in ARPE-19 Cells

ARPE-19 cells stained with an $iPLA_2$-VIA-specific antibody confirmed the location of $iPLA_2$-VIA in the cytosol of the RPE cells (Fig. 2C).

Validation of POS and Latex Bead Uptake by ARPE-19 Cells

ARPE-19 cells were incubated with Alexa-red–labeled POS or beads for 12 and 24 hours. The identity of the fluorescence-labeled cells was confirmed by confocal microscopy revealing perinuclear localization of POS or beads in RPE cells. No staining was evident when nonlabeled POS were added to the cells or when no POS or beads were added to the media (data not shown).

ARPE-19 Phagocytosis of POS

Alexa red–labeled POS ($n = 3$) or latex beads ($n = 3$) were added to ARPE-19 cultures as described in the Methods section. The cells were washed after 1, 2, 4, 6, 8 10, 12, 16, and 24 hours. Maximum absorbance was found 12 hours after addition of both POS (Fig. 4A) and beads (data not shown).

Expression of PLA_2 after POS Phagocytosis

ARPE-19 cells were fed with POS, as described in the Methods section. After 12 and 24 hours of incubation, the cells were harvested and the protein isolated for Western blot analysis. The 70-kDa $iPLA_2$-VIA was upregulated by 1.6-fold after 12 hours ($P < 0.001$, $n = 4$) and 1.7-fold after 24 hours ($P < 0.001$, $n = 4$; Fig. 4B), whereas the 85 kDa $iPLA_2$-VIA was downregulated by 0.2-fold after 12 and 24 hours ($P < 0.05$, $n = 4$). $cPLA_2$-IVA and $iPLA_2$-VIB revealed no significant change in expression after POS phagocytosis ($n = 4$; Fig. 4B).

No change in $iPLA_2$-VIA, $cPLA_2$-IVA or $iPLA_2$-VIB expression was found after phagocytosis of the beads (data not shown).

Downloaded from iovs.arvojournals.org on 04/13/2021

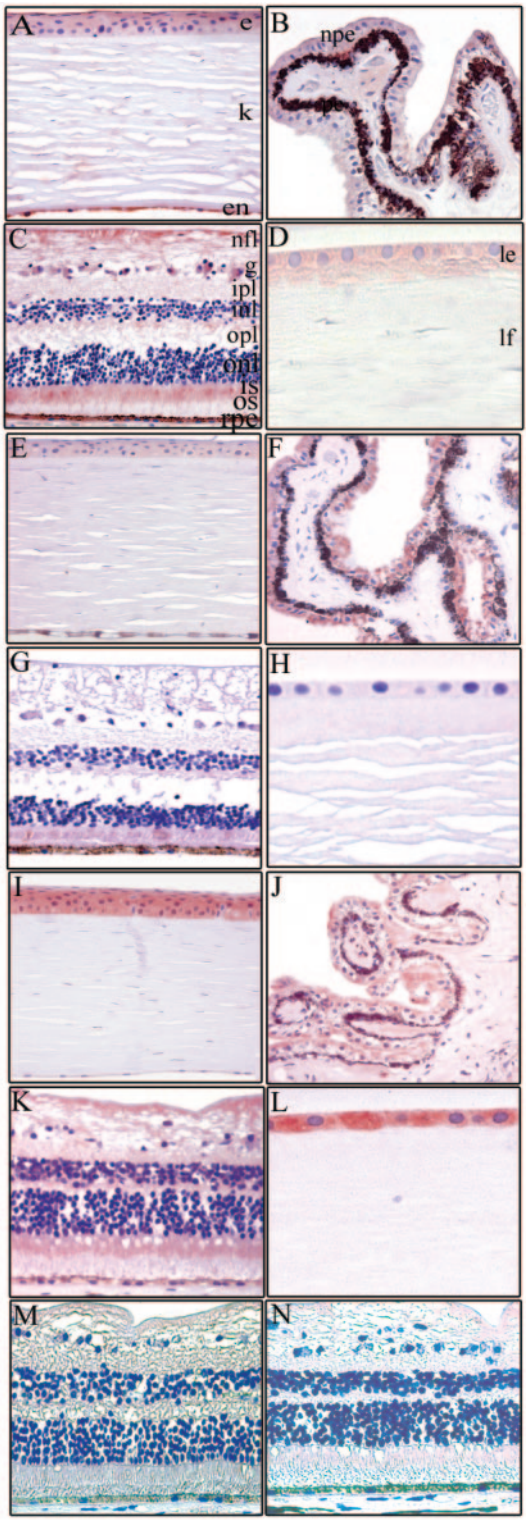

FIGURE 3. Immunohistochemical staining of normal human eyes with antibodies specifically recognizing iPLA$_2$-VIA, cPLA$_2$-IVA, and iPLA$_2$-VIB. (**A–D**) Staining with iPLA$_2$-VIA; (**E–H**) staining with cPLA$_2$-IVA; (**I–L**) staining with iPLA$_2$-VIB; (**M**) staining with rabbit serum. (**N**) Staining with preimmune serum from rabbits used to produce iPLA$_2$-VIB antibody. e, Corneal epithelium; k, corneal keratocytes; en, corneal endothelium; pe, pigmented epithelium; npe, nonpigmented epithelium; nfl, nerve fiber layer; g, ganglion cell layer; ipl, inner plexiform layer; inl, inner nuclear layer; opl, outer plexiform layer; onl, outer nuclear layer; is, photoreceptor inner segments; os, photoreceptor outer segments; POS, photoreceptor outer segments; rpe, retinal pigment epithelium; le, lens epithelium; lf, lens fibers. Magnification: (**A–C**, **E–G**, **I–K**, **M**, **N**) ×200; (**D**, **H**, **L**) ×600.

Induction of iPLA$_2$-VIA Activity by ARPE-19 Phagocytosis of POS

ARPE-19 cultures were fed with POS, and protein was isolated 4, 8, and 12 hours after POS addition. PLA$_2$ activity was measured in conditions with and without POS and was found to be 0.24 micromoles/per milligram protein in untreated ARPE-19 cells ($n = 14$). In ARPE-19 cells fed with POS PLA$_2$, activity was measured to be 0.24 micromoles/per milligram protein ($P < 0.05$, $n = 4$) after 4 hours, 0.34 micromoles/per milligram protein ($P < 0.05$, $n = 4$) after 8 hours, and 0.35 micromoles/per milligram protein ($P < 0.001$, $n = 18$) after 12 hours (Fig. 5A). The iPLA$_2$-VIA-specific inhibitor BEL (10 μM) was added to the proteins to estimate PLA$_2$ activity and was found to inhibit all activity induced by phagocytosis of POS (Fig. 5A). Addition of beads to the ARPE-19 cells did not induce iPLA$_2$-VIA activity, which was measured at 0.23 micromoles/per milligram protein after 12 hours ($n = 8$; Fig. 5A). Inhibition with the specific cPLA$_2$-IVA inhibitor AACOCF3 did not reveal a significant role of cPLA$_2$-IVA in the increased PLA$_2$ activity induced by phagocytosis (not shown).

Inhibition of ARPE-19 Phagocytosis by BEL

The specific iPLA$_2$-VIA inhibitor BEL (10 μM) significantly reduced ARPE-19 phagocytosis of POS (24%; $P < 0.01$, $n = 16$;

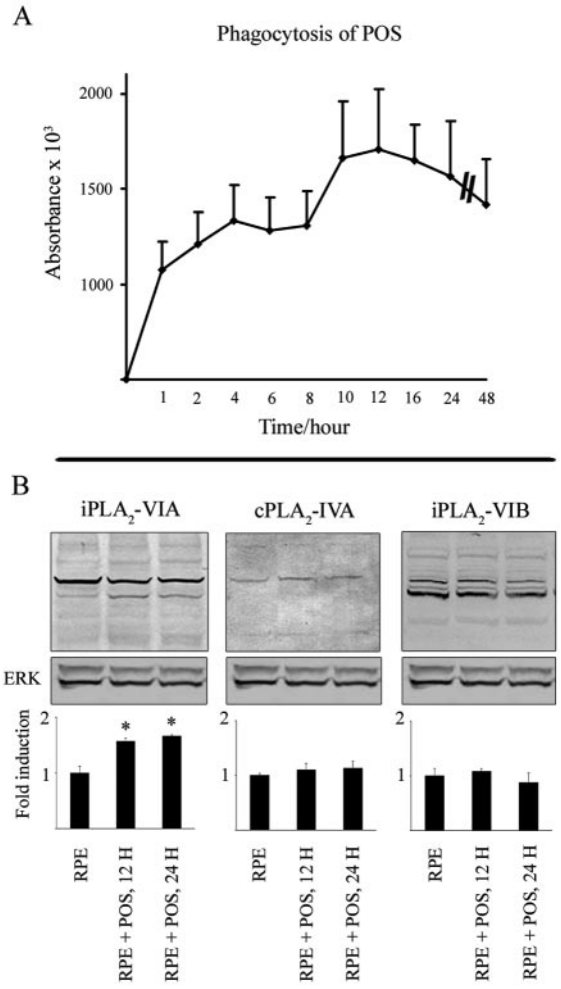

FIGURE 4. (**A**) Fluorescence absorbance at various time points after addition of POS to 3-week-old ARPE-19 cells. (**B**) Western blot analysis, using antibodies against iPLA$_2$-VIA, cPLA$_2$-IVA, and iPLA$_2$-VIB, on protein isolated from ARPE-19 cell before and after POS phagocytosis. ERK staining was used as the loading control. *Significance level $P < 0.05$.

Downloaded from iovs.arvojournals.org on 04/13/2021

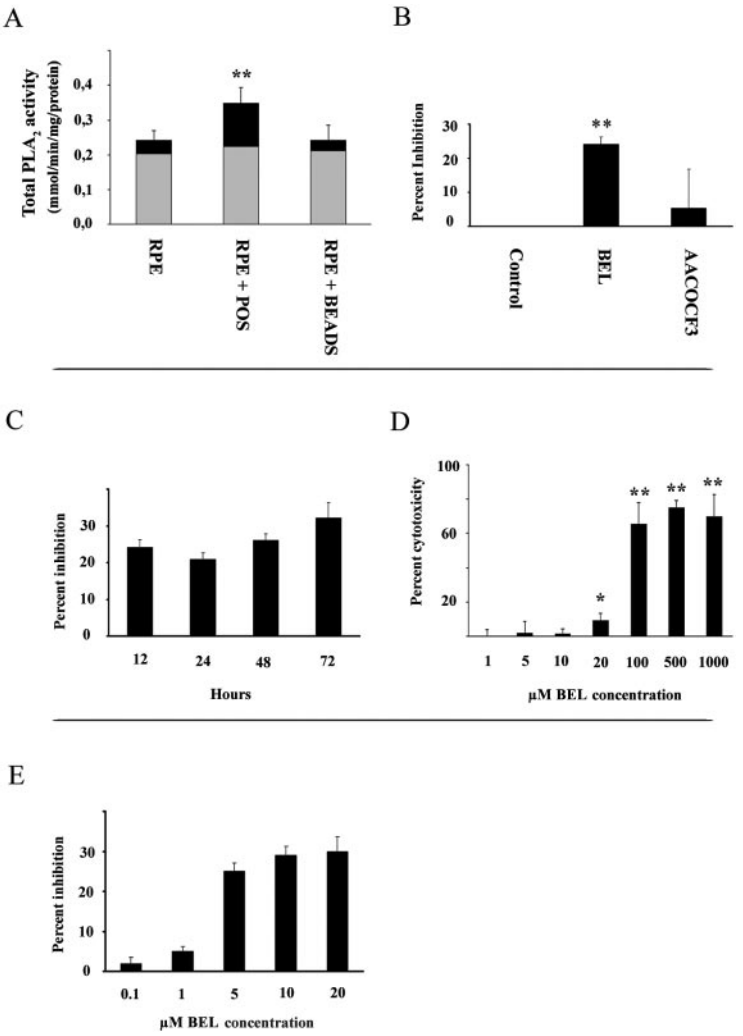

FIGURE 5. (**A**) PLA_2 activity in ARPE-19 cells fed with POS or beads. Bars represent total PLA_2 activity (±SD). *Black* portions indicate $iPLA_2$-VIA-specific activity. (**B**) Inhibition of ARPE-19 phagocytosis of POS by the specific $iPLA_2$-VIA inhibitor BEL (10 μM) or the $cPLA_2$-IVA inhibitor AACOCF3 (10 μM). Bars represent the mean percentage of inhibition (±SD). (**C**) Irreversible inhibition of ARPE-19 phagocytosis of POS 24, 48, and 72 hours after addition of BEL. POS was repeatedly added every 12 hours. Bars represent the mean BEL inhibition (±SD). (**D**) Cytotoxicity of various concentrations of BEL using an MTT assay. Bars represent the mean percentage of cytotoxicity after addition of the different BEL concentrations (±SD). (**E**) Inhibition of ARPE-19 phagocytosis of POS by different BEL concentrations. Bars represent mean percentage of inhibition (±SD). Significance levels: $^*P < 0.05$, $^{**}P < 0.001$.

Fig. 5B). The inhibition was sustained after readdition of POS after 24, 48, and 72 hours (21%; $P < 0.05$, $n = 4$), 26% ($P < 0.05$, $n = 4$), and 32% ($P < 0.05$, $n = 4$), respectively (Fig. 5C). BEL toxicity was evaluated by MTT as described in the Methods section. Significant toxicity was observed when cells were exposed to BEL concentrations above 20 μM (Fig. 5D). BEL concentrations between 5 and 20 μM had an equal inhibitory effect on ARPE-19 phagocytosis of POS (Fig. 5E). The $cPLA_2$-IVA inhibitor AACOCF3 ($n = 15$; Fig. 5B) and propranolol ($n = 15$; data not shown) did not significantly reduce phagocytosis.

Discussion

RPE phagocytosis of POS is essential for retinal function, and it has been suggested that alterations in POS degradation may lead to age-related macular degeneration (AMD), the most common cause of irreversible blindness in the Western world.[21,22] Besides phagocytizing POS, RPE cells have various additional physiological functions such as supporting the neuroretina, creating part of the blood–brain barrier, and transporting metabolites and water.[23] Studies of other phagocytizing cells may be helpful in understanding RPE phagocytosis of POS. PLA_2 activity has been demonstrated in macrophages, and it has been shown that PLA_2 activity increases during phagocytosis. Among other specific PLA_2 subtypes, $iPLA_2$-VIA has been shown to be essential in macrophage phagocytosis.[7,9,24,25] Lyso-phosphatidylcholine, a metabolite of $iPLA_2$-VIA activity, seems to generate a signal for phagocytosis, and macrophage phagocytosis can be inhibited by the $iPLA_2$-specific inhibitor BEL.[9] Evidence on $cPLA_2$-IVA involvement in macrophage phagocytosis has also been suggested,[13,26] whereas no studies have explored a role of $iPLA_2$-VIB in phagocytosis.

In the retina, the literature has described PLA_2 activity in the RPE cells as well as in the neuroretina. However, no specific PLA_2 has been identified in these tissues, and the current knowledge is based on indirect evidence of substrate-specific PLA_2 activity.[16,17,27] Based on the previous findings, the purpose of this study was to identify intracellular PLA_2 in the human eye, with emphasis on the outer retinal layers, and to evaluate the role of intracellular PLA_2 in RPE phagocytosis of POS. Intracellular PLA_2 expression was found in various parts of the eye, as outlined in Table 2. Abundant expression of genes encoding $iPLA_2$-VIA were present in the human ARPE-19 cell line, whereas RPE expression of $cPLA_2$-IVA and $iPLA_2$-VIB was less abundant (Fig. 1A). The various known splice variants of $iPLA_2$-VIA were identified, including a new splice variant without exon 4, which creates a frameshift and thereby a new possible regulator of $iPLA_2$-VIA activity (Fig. 1B). Because all splice variants of $iPLA_2$-VIA seem to be present in the ARPE-19 cells, there may be tightly regulated functions of $iPLA_2$-VIA, not only in the phagocytosis of POS but also in other functions of these multifunctional cells. However, the physiological relevance of the splice variants remains to be shown.

On the protein level, expression of $iPLA_2$-VIA, $cPLA_2$-IVA, and $iPLA_2$-VIB were identified, both in the normal human eye sections and the ARPE-19 cells (Fig. 2). Western blot analysis of

Downloaded from iovs.arvojournals.org on 04/13/2021

iPLA$_2$-VIA revealed ~85- and ~70-kDa bands. The ~85-kDa band has been shown to be a catalytically active iPLA$_2$-VIA, and evidence from pancreatic islets and insulinoma cells shows the significance of the ~70 kDa iPLA$_2$-VIA.[28] In the present study the specificity of the ~70 kDa band was furthermore strengthened by immunoprecipitation.

The ~70 kDa band of iPLA$_2$-VIA was upregulated 12 and 24 hours after the addition of POS to ARPE-19 cells indicating a role in RPE phagocytosis. It has been suggested that the high-molecular-weight iPLA$_2$ is proteolytically cleaved to create the low-molecular-weight iPLA$_2$.[29] Because the present Western blot analysis reveals decreased expression of the high-molecular-weight iPLA$_2$-VIA in phagocytizing ARPE-19 cells, the induction of the ~70-kDa band may be due to cleavage of the ~85-kDa band. Furthermore, the ~85-kDa band has been shown to include a membrane-binding site,[28] and it is therefore tempting to suggest that cleavage possibly leads to the smaller ~70-kDa band, which may relocalize and thereby obtain ability to act in the phagocytosis process. Future studies are necessary, however, to clarify these issues.

Previous studies have shown a role of COX-2 in rat RPE phagocytosis and it is possible that cPLA$_2$-IVA may play a role in this induction.[18] However, no significant upregulation of cPLA$_2$-IVA was found (Fig. 4B) and the present study could not confirm an involvement of this subtype in RPE phagocytosis of POS. Finally, no significant regulation of iPLA$_2$-VIB was observed (Fig. 4B). Involvement of sPLA$_2$ in macrophage phagocytosis has previously been shown[7,15,26] and this subgroup of PLA$_2$ may also be involved in RPE phagocytosis of POS. However, the present study did not evaluate possible roles of sPLA$_2$, and future studies should investigate this question. In comparison with published data on PLA$_2$ activity in different cell types, basal PLA$_2$ activity in ARPE-19 cells appears to be relatively high.[30,31] In the present study, we showed increased PLA$_2$ activity in phagocytosing RPE cells 8 (not shown) and 12 hours (Fig. 5A) after ARPE-19 cells were fed with POS, whereas no upregulation was seen 4 hours after addition of POS. The delay on increased PLA$_2$ activity suggests that PLA$_2$ activity may be a response to POS engulfment and thereby a mechanism to degrade the membranes and thereby regulate phagocytosis. Of interest, the increased activity could be blocked by BEL, which strongly supports the role of iPLA$_2$-VIA in RPE phagocytosis of POS (Figs. 5B, 5C). When inhibiting phagocytosis with the iPLA$_2$-VIA specific inhibitor BEL, we significantly reduced phagocytosis, whereas no effect was found with the cPLA$_2$-IVA-specific inhibitor AACOCF3. Because PLA$_2$-VIA activity has been implicated in the involvement of normal phospholipid remodeling and several reports have suggested that iPLA$_2$-VIA is one of the main modulators of PC catabolism, our present data support this hypothesis.[32,33]

In conclusion, in the present study, we explored intracellular PLA$_2$ in the human retina. We confirmed that RPE elicits PLA$_2$ activity and identified iPLA$_2$-VIA, cPLA$_2$-IVA, and iPLA$_2$-VIB on both the mRNA and the protein levels. We report a significant role of iPLA$_2$-VIA in RPE phagocytosis of POS, whereas cPLA$_2$-IVA and iPLA$_2$-VIB do not seem to be essential in this process. Because RPE phagocytosis is critical for vision and is damaged during pathologic processes such as AMD, it is tempting to suggest that iPLA$_2$-VIA could be a target for future pharmacological intervention.

Acknowledgments

The authors thank Sven Erik Nilsson and Staffan Sundelin for valuable help with the isolation and labeling of POS.

References

1. Hall MO. Phagocytosis of light- and dark-adapted rod outer segments by cultured pigment epithelium. *Science*. 1978;202:526–528.
2. Collins FD, Love RM, Morton RA. Studies in rhodopsin. V. Chemical analysis of retinal material. *Biochem J*. 1952;51:669–673.
3. Fleischer S, McConnell DG. Preliminary observations on the lipids of bovine retinal outer segment disks. *Nature*. 1966;212:1366–1367.
4. Anderson RE, Maude MB. Phospholipids of bovine outer segments. *Biochemistry*. 1970;9:3624–3628.
5. Martin RE, Elliott MH, Brush RS, Anderson RE. Detailed characterization of the lipid composition of detergent-resistant membranes from photoreceptor rod outer segment membranes. *Invest Ophthalmol Vis Sci*. 2005;46:1147–1154.
6. Irschick EU, Sgonc R, Bock G, et al. Retinal pigment epithelial phagocytosis and metabolism differ from those of macrophages. *Ophthalmic Res*. 2004;36:200–210.
7. Lennartz MR. Phospholipases and phagocytosis: the role of phospholipid-derived second messengers in phagocytosis. *Int J Biochem Cell Biol*. 1999;31:415–430.
8. Suram S, Brown GD, Ghosh M, et al. Regulation of cytosolic phospholipase A2 activation and cyclooxygenase 2 expression in macrophages by the beta-glucan receptor. *J Biol Chem*. 2006;281:5506–5514.
9. Perez R, Balboa MA, Balsinde J. Involvement of group VIA calcium-independent phospholipase A2 in macrophage engulfment of hydrogen peroxide-treated U937 cells. *J Immunol*. 2006;176:2555–2561.
10. Valentin E, Lambeau G. Increasing molecular diversity of secreted phospholipases A(2) and their receptors and binding proteins. *Biochim Biophys Acta*. 2000;1488:59–70.
11. Kudo I, Murakami M. Phospholipase A2 enzymes. *Prostaglandins Other Lipid Mediat*. 2002;68–69:3–58.
12. Six DA, Dennis EA. The expanding superfamily of phospholipase A(2) enzymes: classification and characterization. *Biochim Biophys Acta*. 2000;1488:1–19.
13. Girotti M, Evans JH, Burke D, Leslie CC. Cytosolic phospholipase A2 translocates to forming phagosomes during phagocytosis of zymosan in macrophages. *J Biol Chem*. 2004;279:19113–19121.
14. Zaitseva L, Vaisburd M, Shaposhnikova G, Mysyakin E. Role of eicosanoids in regulation of macrophage phagocytic functions by platelet-activating factor during endotoxic shock. *Bull Exp Biol Med*. 2000;130:879–881.
15. Balestrieri B, Hsu VW, Gilbert H, et al. Group V secretory phospholipase A2 translocates to the phagosome after zymosan stimulation of mouse peritoneal macrophages and regulates phagocytosis. *J Biol Chem*. 2006;281:6691–6698.
16. Van TC, Jacob M, Salesse C. Human retinal pigment epithelium secretes a phospholipase A2 and contains two novel intracellular phospholipases A2. *Biochem Cell Biol*. 2001;79:1–10.
17. Jacob M, Weech PK, Salesse C. Bovine retinal pigment epithelium contains novel types of phospholipase A2. *Biochem J*. 1997;327:455–460.
18. Ershov AV, Bazan NG. Induction of cyclooxygenase-2 gene expression in retinal pigment epithelium cells by photoreceptor rod outer segment phagocytosis and growth factors. *J Neurosci Res*. 1999;58:254–261.
19. Schraermeyer U, Stieve H. A newly discovered pathway of melanin formation in cultured retinal pigment epithelium of cattle. *Cell Tissue Res*. 1994;276:273–279.
20. Larsson PK, Claesson HE, Kennedy BP. Multiple splice variants of the human calcium-independent phospholipase A2 and their effect on enzyme activity. *J Biol Chem*. 1998;273:207–214.
21. Rakoczy PE, Zhang D, Robertson T, et al. Progressive age-related changes similar to age-related macular degeneration in a transgenic mouse model. *Am J Pathol*. 2002;161:1515–1524.
22. Finnemann SC, Leung LW, Rodriguez-Boulan E. The lipofuscin component A2E selectively inhibits phagolysosomal degradation of photoreceptor phospholipid by the retinal pigment epithelium. *Proc Natl Acad Sci USA*. 2002;99:3842–3847.

Downloaded from iovs.arvojournals.org on 04/13/2021

23. Strauss O. The retinal pigment epithelium in visual function. *Physiol Rev*. 2005;85:845–881.
24. Karimi K, Gemmill TR, Lennartz MR. Protein kinase C and a calcium-independent phospholipase are required for IgG-mediated phagocytosis by Mono-Mac-6 cells. *J Leukoc Biol*. 1999;65:854–862.
25. McNally AK, Anderson JM. Multinucleated giant cell formation exhibits features of phagocytosis with participation of the endoplasmic reticulum. *Exp Mol Pathol*. 2005;79:126–135.
26. Shirai Y, Balsinde J, Dennis EA. Localization and functional interrelationships among cytosolic group IV, secreted group V, and Ca2+-independent group VI phospholipase A2s in P388D1 macrophages using GFP/RFP constructs. *Biochim Biophys Acta*. 2005;1735:119–129.
27. Castagnet PI, Roque ME, Pasquare SJ, Giusto NM. Phosphorylation of rod outer segment proteins modulates phosphatidylethanolamine N-methyltransferase and phospholipase A2 activities in photoreceptor membranes. *Comp Biochem Physiol B Biochem Mol Biol*. 1998;120:683–691.
28. Tanaka H, Takeya R, Sumimoto H. A novel intracellular membrane-bound calcium-independent phospholipase A(2). *Biochem Biophys Res Commun*. 2000;272:320–326.
29. Ramanadham S, Song H, Hsu FF, et al. Pancreatic islets and insulinoma cells express a novel isoform of group VIA phospholipase A2 (iPLA2 beta) that participates in glucose-stimulated insulin secretion and is not produced by alternate splicing of the iPLA2 beta transcript. *Biochemistry*. 2003;42:13929–13940.
30. Zhang L, Peterson BL, Cummings BS. The effect of inhibition of Ca2+-independent phospholipase A2 on chemotherapeutic-induced death and phospholipid profiles in renal cells. *Biochem Pharmacol*. 2005;70:1697–1706.
31. Yang HC, Mosior M, Ni B, Dennis EA. Regional distribution, ontogeny, purification, and characterization of the Ca2+-independent phospholipase A2 from rat brain. *J Neurochem*. 1999;73:1278–1287.
32. Barbour SE, Kapur A, Deal CL. Regulation of phosphatidylcholine homeostasis by calcium-independent phospholipase A2. *Biochim Biophys Acta*. 1999;1439:77–88.
33. Manguikian AD, Barbour SE. Cell cycle dependence of group VIA calcium-independent phospholipase A2 activity. *J Biol Chem*. 2004;279:52881–52892.

Downloaded from iovs.arvojournals.org on 04/13/2021